Available online at www.sciencedirect.com
ScienceDirect
Polymer 48 (2007) 6426–6433
polymer
www.elsevier.com/locate/polymer

High impact strength epoxy nanocomposites with natural nanotubes

Yueping Ye [a], Haibin Chen [a], Jingshen Wu [a,*], Lin Ye [b]

[a] Department of Mechanical Engineering, The Hong Kong University of Science and Technology (HKUST), Hong Kong, China
[b] School of Aerospace, Mechanical and Mechatronic Engineering, University of Sydney, NSW 2006, Australia

Received 9 April 2007; received in revised form 26 July 2007; accepted 15 August 2007
Available online 19 August 2007

Abstract

Epoxy-based nanocomposites were prepared with natural nanotubes from halloysite, a clay mineral with the empirical formula $Al_2Si_2O_5(OH)_4$. The morphology of the nanotubes was examined by scanning electron microscopy (SEM) and transmission electron microscopy (TEM) and was found geometrically similar to multi-walled carbon nanotubes. The thermal and mechanical properties of the nanocomposites were characterized by thermogravimetric analysis, dynamic mechanical analysis, Charpy impact and three-point bending tests. The results demonstrated that blending epoxy with 2.3 wt% halloysite nanotubes increased the impact strength by 4 times without scarifying flexural modulus, strength and thermal stability. Unique toughening mechanisms for this improvement were investigated and discussed. It was proposed that impact energy was dissipated via the formation of damage zones with a large number of micro-cracks in front of the main crack. The micro-cracks were stabilized by nanotube bridging. Nanotube bridging, pull-out and breaking were also observed and proposed as the major energy dissipating events. The findings of this work suggest that halloysite nanotube may be an effective impact modifier for epoxy and other brittle polymers.

Keywords: Halloysite nanotube; Impact strength; Epoxy

1. Introduction

How to toughen brittle polymers without scarifying other important properties is a long-standing challenge. Substantial toughening, particularly for brittle polymers, such as polystyrene, poly(methyl methacrylate) and epoxies, is usually achieved by adding rubbery modifiers, where fracture energy is dissipated via plastic deformation of the matrix induced by rubber particles [1,2]. Two well-accepted toughening mechanisms are multiple crazing [3] and massive shear banding [4]. The former is widely seen in blends where the matrix prefers to craze such as in high impact polystyrene (HIPS). The rubber particles in HIPS have two important functions. Firstly, under an applied load, the rubber particles act as triaxial stress concentrators and promote craze formation in the elevated stress zones in the vicinity of the particles. Secondly, the rubber particles are craze terminators, preventing the growth of the crazes into cracks [3]. Thus, a large number of small crazes are generated and stabilized. This process leads to high energy absorption during HIPS fracture. Highly crosslinked polymers such as epoxies are toughened by rubbers via matrix shear banding [4,5]. Though epoxy resins can be toughened effectively by rubbers, addition of rubber also results in a decrease in other desirable mechanical and physical properties including modulus, strength and thermal stability [6–8]. Rigid micro-sized inorganic [9,10] or organic [11,12] modifiers were employed in modification of brittle polymers, aiming to synergistic improvement in both toughness and rigidity. Published work, however, shows that toughening efficiency of rigid micro-sized particles is much lower than that of rubbers due to various reasons, including that rigid particles cannot effectively stabilize/stop crack propagation.

Motivated by recent developments in nanocomposite technology [13], toughening epoxies using inorganic nanofillers has been attempted. For example, organically modified montmorillonite (MMT) has been widely investigated as a candidate

* Corresponding author. Tel.: +852 2358 7200; fax: +852 2358 1543.
E-mail address: mejswu@ust.hk (J. Wu).

0032-3861/$ - see front matter © 2007 Elsevier Ltd. All rights reserved.
doi:10.1016/j.polymer.2007.08.035

for toughness enhancement of polymers. It is anticipated that the layered nanostructure of MMT would have some nano-size effects once MMT is exfoliated and dispersed homogenously in a polymer matrix. Successful examples show that when a MMT nanocomposite is subjected to a load, micro-cracks form between two weakly bonded clay layers and the growth of the micro-cracks is later stopped by the MMT platelets nearby, which leads to higher impact energy [14,15]. Carbon nanotube (CNT) is also considered as an ideal modifier for polymer modification due to its excellent mechanical strength and large aspect ratio. Extensive efforts have been made in developing epoxy/CNT nanocomposites with improved toughness [16–18]. For instance, the amino-functionalized multi-walled CNT (MWCNT) doubled the impact strength of an epoxy [16]. Considering the extremely high cost and the difficulties in preparation of CNTs and polymer/CNT nanocomposites, the way of industrializing CNT-based nanocomposites on a large scale is still long.

Halloysite is a clay mineral with the empirical formula $Al_2Si_2O_5(OH)_4$ consisting of numerous numbers of nanotubes. Potential applications of halloysite nanotubes (HNTs) for drug-delivery were previously discussed in open literature [19–21]. Given the geometrical similarity between HNT and MWCNT, HNT is expected to be an effective impact modifier for brittle polymers at a much lower cost. In this work, we report the mechanical and physical properties, microstructure and toughening mechanisms of a nanocomposite prepared in our lab based on an epoxy resin and HNTs.

2. Experimental

2.1. Preparation of nanocomposites

The nanocomposites were prepared using halloysite (Imerys Tableware New Zealand Limited), EPON Resin 828 (Bisphenol A epoxy, Resolution Performance Products) with curing agent 4,4′-methylene dianiline (MDA, Aldrich) at a 100/27 weight ratio. The preparation process was similar to solution intercalation of layered silicate into polymers [22,23]. In brief, halloysite was first dispersed in acetone and mechanically stirred for 30 min at room temperature. The solution was then introduced into the epoxy resin and stirred for another 2 h at 75 °C. After degassing, MDA was added with gentle mixing. The mixture was then poured into a steel mold for curing. The curing condition was set as: pre-cure at 80 °C for 2 h and post-cure at 160 °C for another 2 h.

2.2. Materials' characterization

The morphologies of halloysite and epoxy/halloysite nanocomposites were examined using a Leitz-labor Lux microscope, SEM (JEOL JSM-6700F) and TEM (JEOL JEM-2010 for halloysite and JEOL 100CX for nanocomposites). The TEM samples of the nanocomposites were cut with an ultramicrotome (Leica ultracut-R) and the thickness of the TEM samples was in the range of 80–100 nm. X-ray diffraction (XRD) measurements were performed on Philips PW1830 using Cu Kα radiation with a wavelength of 0.154 nm. The scanning range was from 2° to 15° at a rate of 0.025°/s and a step of 0.05°.

Dynamic mechanical property was measured using Perkin–Elmer 7e DMA in three-point bending mode at a frequency of 1 Hz. The specimen dimension was $18.0 \times 3.0 \times 0.5\ mm^3$. The temperature was varied from 30 °C to 220 °C at 10 °C/min under helium atmosphere at a flow rate of 20 ml/min. The thermal decomposition temperatures were determined using Perkin–Elmer TGA7 from 20 °C to 750 °C at 10 °C/min under nitrogen atmosphere at a flow rate of 20 ml/min. For each sample at least two specimens were tested under the same conditions.

2.3. Mechanical tests

The flexural modulus of the nanocomposites was determined according to ASTM D790 on a universal testing machine (MTS Alliance RT/10). The specimens with the geometry of $70.0 \times 2.7 \times 3.0\ mm^3$ were bended with a support span of 50.0 mm at a crosshead speed of 1.3 mm/min. Notched Charpy impact tests were performed according to ASTM D5942 on an impact tester (CEAST) with pendulum energy of 0.5 J and a span of 60.0 mm. The specimen size was $70.0 \times 10.0 \times 3.0\ mm^3$, cut from the mold sheet. A 45° V-shaped notch was made at the central part of the impact bar by a razor notching machine (CEAST) with a notch-tip radius of 0.25 mm. Before the mechanical tests, all the samples were annealed at 180 °C (10 °C above T_g) for 2 h to eliminate residual stress caused by cutting. For each nanocomposite sample, at least five specimens were tested. In addition, the fracture surface of the broken specimens was examined with SEM.

To study the fracture behaviour and toughening mechanisms of the epoxy/halloysite nanocomposites, single-edge-single-notched 3-point-bend (SESN-3PB) tests were conducted. The configuration of the specimen was the same as that for Charpy impact test. A sharp pre-crack was produced by tapping a fresh razor blade into the tip of a saw-made notch. The test condition was the same as that for flexural bending tests but with a lower crosshead speed of 0.1 mm/min. To investigate the crack initiation process, the loading was stopped before the stress reached the fracture strength. The block containing the arrested crack tip was then cut and trimmed to the middle section [24–26]. SEM was applied to examine this area.

3. Results and discussion

3.1. Microstructure

Fig. 1 depicts the SEM and TEM micrographs of HNTs. Evidently, these nanotubes have a tubular morphology, geometrically similar to multi-walled CNT. The outer diameters of HNTs are generally smaller than l00 nm and the length ranges from 500 nm to l600 nm. Unlike CNTs, which always have an entangled structure, these nanotubes are straight with no entanglement, which makes HNTs' dispersion in viscous

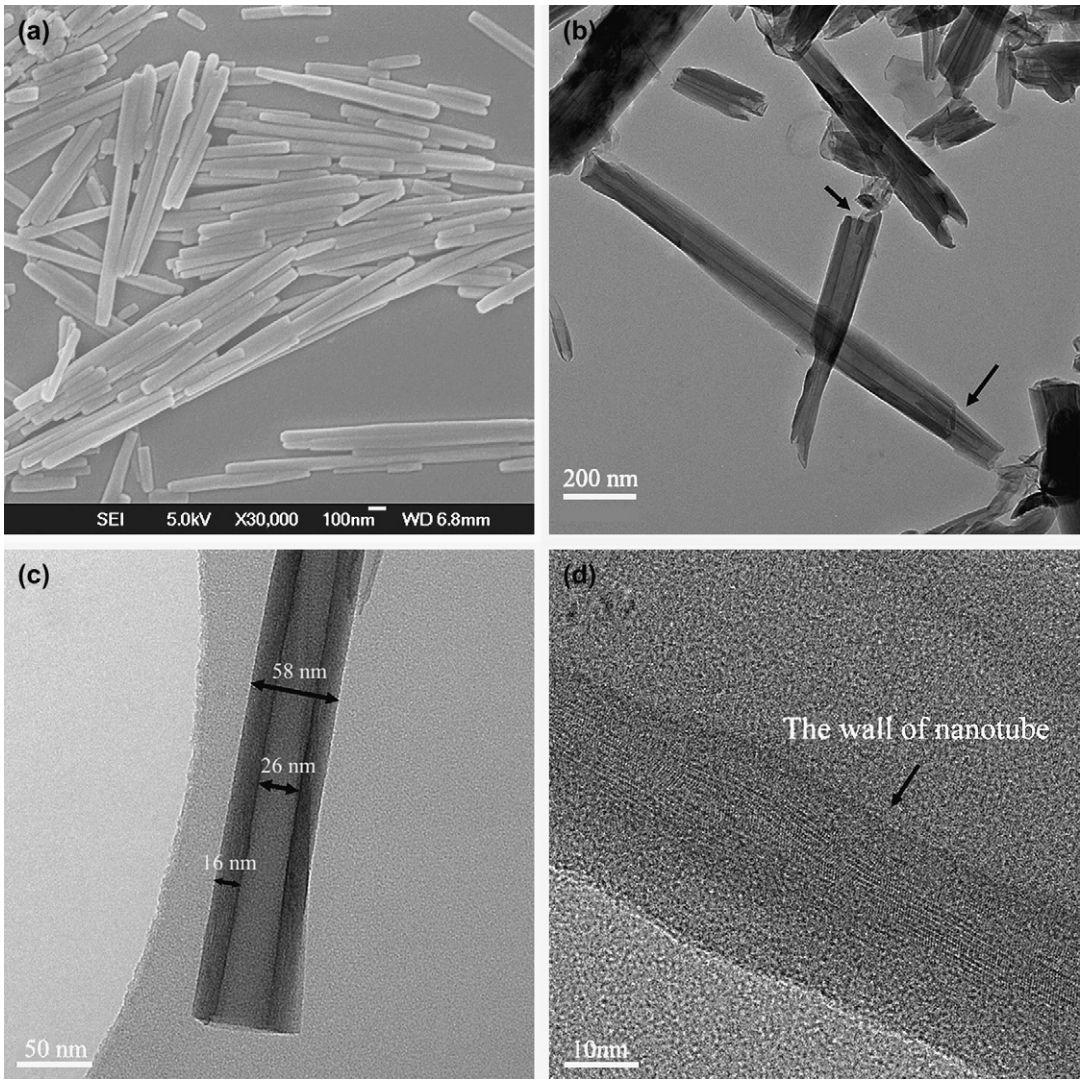

Fig. 1. Electron micrographs of halloysite: (a) and (b) the entire view, (c) TEM micrograph of an HNT, (d) TEM micrograph showing the wall of a nanotube with a multi-layer structure.

polymer matrix easier compared with CNTs. Moreover, the wall thickness is around 20 nm. According to X-ray diffraction analysis, the interlayer distance is about 7–10 Å. Thus there are tens of layers in the wall, agreeing with our TEM findings shown in Fig. 1d.

The microstructure of the epoxy/HNT nanocomposites was examined with electron and optical microscopies. As revealed in Figs. 2 and 3, HNTs were well dispersed in the epoxy but in two different dispersion ways. Some HNTs were randomly dispersed in the matrix with large inter-tube distance, forming the epoxy-rich region (see Figs. 2a and 3a); while the other HNT tubes dispersed in the matrix with much short inter-tube distance, which results in the formation of an HNT-rich region (see Figs. 2b and 3b). Though the HNT-rich region looks like clusters of HNTs, a closer examination of the HNT-rich regions by TEM, Fig. 3b, shows that the spaces among the HNTs were actually filled by epoxy. The dark circular dots of ~100 nm in Fig. 3b are the images of the HNT ends. In summary, the morphology of the epoxy/HNT nanocomposites prepared in this work has two phases (see Fig. 4). The epoxy-rich region is the continuous phase and the discontinuous phase is the HNT-rich regions, which can be regarded as the rigid, high content HNT composite particles embedded in the continuous phase. It will be demonstrated in the later part of this paper that this morphology played an important role in toughening the nanocomposites.

The microstructure changes of the HNT after it was incorporated in the nanocomposites were studied by XRD and are shown in Fig. 5. For the pristine halloysite two diffraction peaks were seen at 8.8° and 12.0°, respectively. The former was associated with hydrated HNTs with a layer distance of 10 Å; the latter was associated with dehydrated HNTs corresponding to a layer distance of 7 Å [27]. After the HNTs formed nanocomposites, only one diffraction peak was detected at 12.0°. This phenomenon suggests that the hydrated HNTs were dehydrated during the preparation processes of the nanocomposites, most likely, due to the loss of interlayer water in the curing process of the epoxy. In addition, the

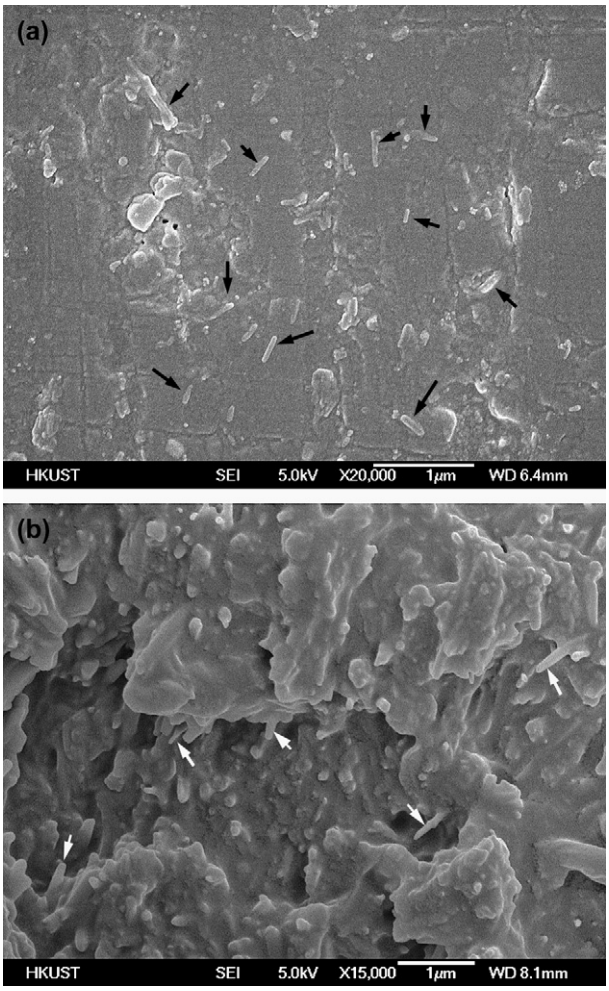

Fig. 2. SEM micrographs of epoxy nanocomposite with 2.3 wt% halloysite in: (a) the epoxy-rich region and (b) the HNT-rich region.

HNTs in the nanocomposites seemed not to be intercalated by the epoxy.

3.2. Thermal and mechanical property

Fig. 6 represents the TGA data of the nanocomposites. Owing to the incorporation of HNTs, the maximum thermal decomposition temperatures (T_ds) of the nanocomposites increased from ~393 °C to as high as ~416 °C at a halloysite loading of 1.6 wt%. This improvement in thermal stability is comparable with silica-modified epoxy systems [28], but different from single-walled CNT-modified epoxy systems reported by Miyagawa and Drzal [29]. The underlying mechanism governing the increase in T_d needs further investigations. The glass transition temperatures (T_gs) of the neat epoxy and the nanocomposites were determined using DMA. As shown in Fig. 7, the T_g of the nanocomposites from the tan δ peaks decreased marginally. The change in T_g associated with the incorporation of inorganic fillers was previously reported and proposed by others [30–33] to be a result of two competitive factors, i.e. rigid-phase reinforcement and destroying of the epoxy network structure.

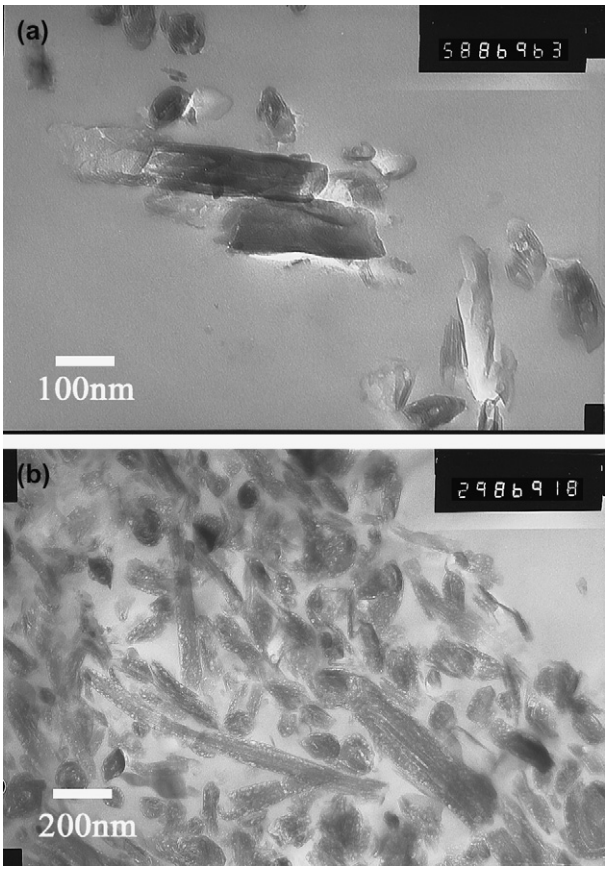

Fig. 3. TEM micrographs of epoxy nanocomposite with 2.3 wt% halloysite in: (a) the epoxy-rich region and (b) the HNT-rich region.

Impact strength of the epoxy/HNT nanocomposites is shown in Fig. 8. To our surprise, adding merely 2.3 wt% HNTs into the epoxy increased its impact strength by 4 times from 0.54 kJ/m^2 (neat epoxy) to 2.77 kJ/m^2 (the nanocomposite). Such a great improvement is comparable to the toughening effect of rubbers [34], but the HNT toughening was achieved at a much lower filler concentration. Moreover, using rubbers to toughen a polymer always scarifies other desirable properties such as modulus, strength and heat resistance [6]. For the current HNT-modified epoxy, the flexural modulus

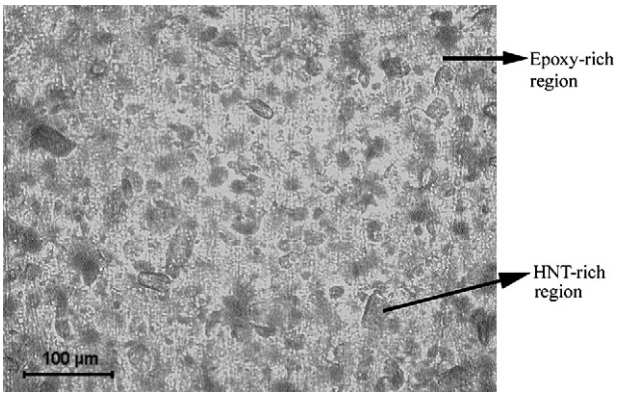

Fig. 4. Optical micrograph showing the two-phase structure of epoxy/HNT nanocomposite.

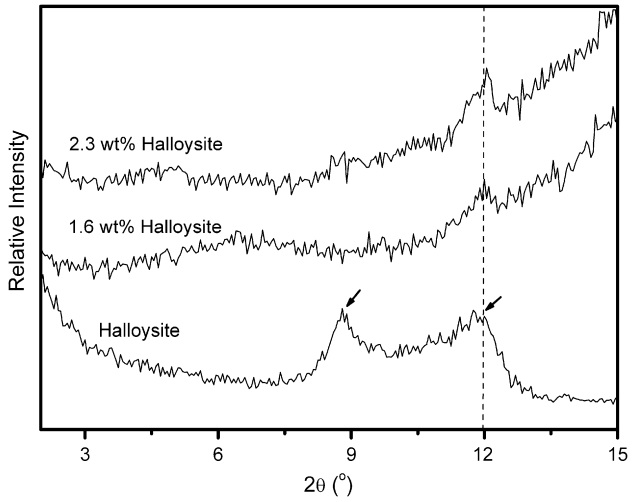

Fig. 5. X-ray diffraction patterns of halloysite powder and the fully cured epoxy/HNT nanocomposites.

and strength even had slight increases (see Fig. 8). From this point of view, HNT is much superior to rubbers as an impact modifier. Compared with other inorganic nanofiller modified epoxy nanocomposites reported in the literature, the toughening effect of HNTs is still very impressive. For example, the impact strength was improved by ~60% using 3 wt% MMT in epoxy/MMT nanocomposites [35] and ~35% using 4 vol% TiO_2 nanoparticles in epoxy/TiO_2 nanocomposites [36]. Given the observed substantial improvement in impact strength from HNTs, ~400%, it is worthwhile to conduct a thorough study on the toughening mechanisms behind the phenomena.

3.3. Toughening mechanism

To investigate the toughening mechanisms, the fracture surfaces of the broken specimens after the impact tests were examined using a high resolution SEM. As revealed in Fig. 9a, nanotube debonding/pull-out is clearly seen in the crack initiation region of fracture surface. However, the toughening contribution from the nanotube debonding/pull-out associated with the propagation of the main crack should not be the dominant one. According to the calculation done by Cooper et al. [37], the energy for pulling out MWCNT is less than 37 J/m^2. Considering that the fracture surface area generated by the main crack propagation is small, additional energy dissipation by nanotube debonding/pull-out taking place during the main crack propagation should be insignificant.

Besides nanotube debonding/pull-out on the main fracture surfaces, huge numbers of micro-cracks were found on the fracture surfaces. The length of the micro-cracks was in a range from 100 nm to nearly 1 μm. Moreover, the micro-cracks were bridged by nanotubes. From the micrograph in Fig. 9b, it can be seen that several nanotubes bridge the two surfaces of a micro-crack with a gap of about 600 nm. Because of nanotube bridging, the micro-cracks were stabilized and stopped developing into large and harmful cracks. This observation also suggests that the adhesion between the HNTs and the matrix was quite strong. Some bridging HNTs broke when the crack-opening force exceeded their fracture strength. Similar to the

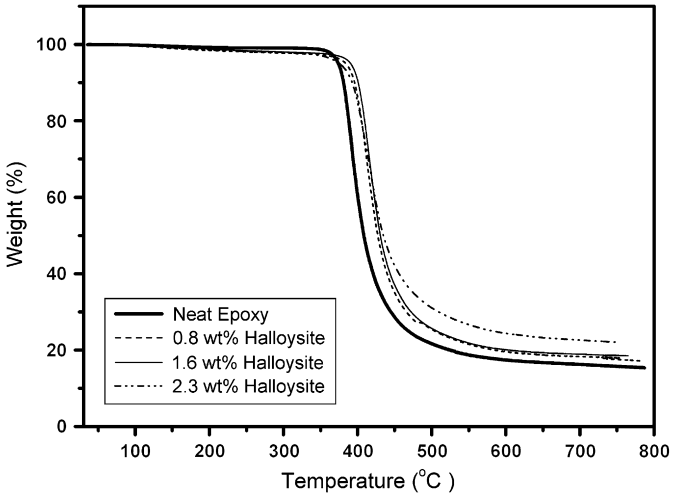

Fig. 6. Thermogravimetric curves of neat epoxy and the epoxy/HNT nanocomposites.

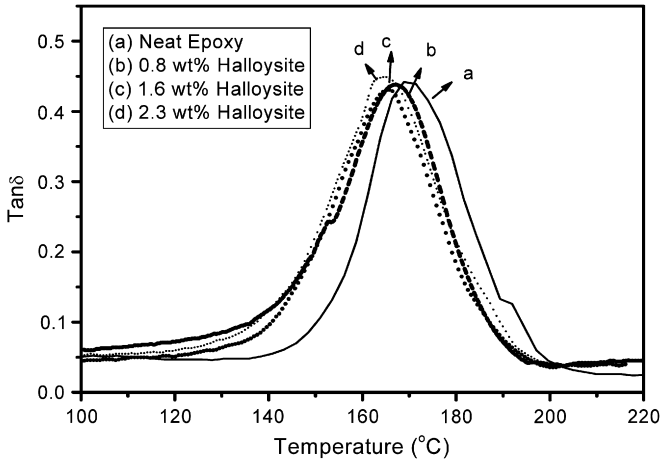

Fig. 7. Dynamic mechanical properties of the nanocomposites with different halloysite loadings.

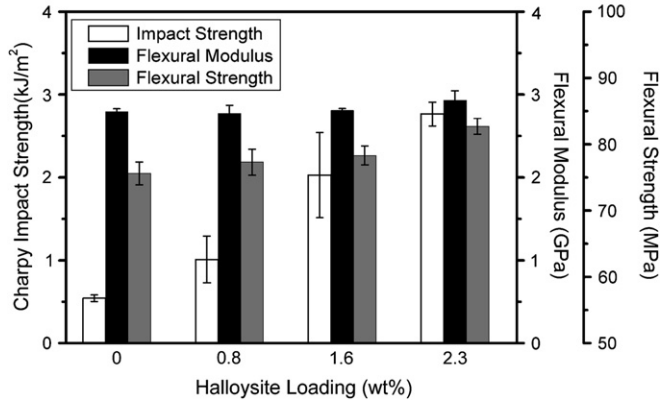

Fig. 8. Mechanical properties of neat epoxy and the nanocomposites with different halloysite loadings.

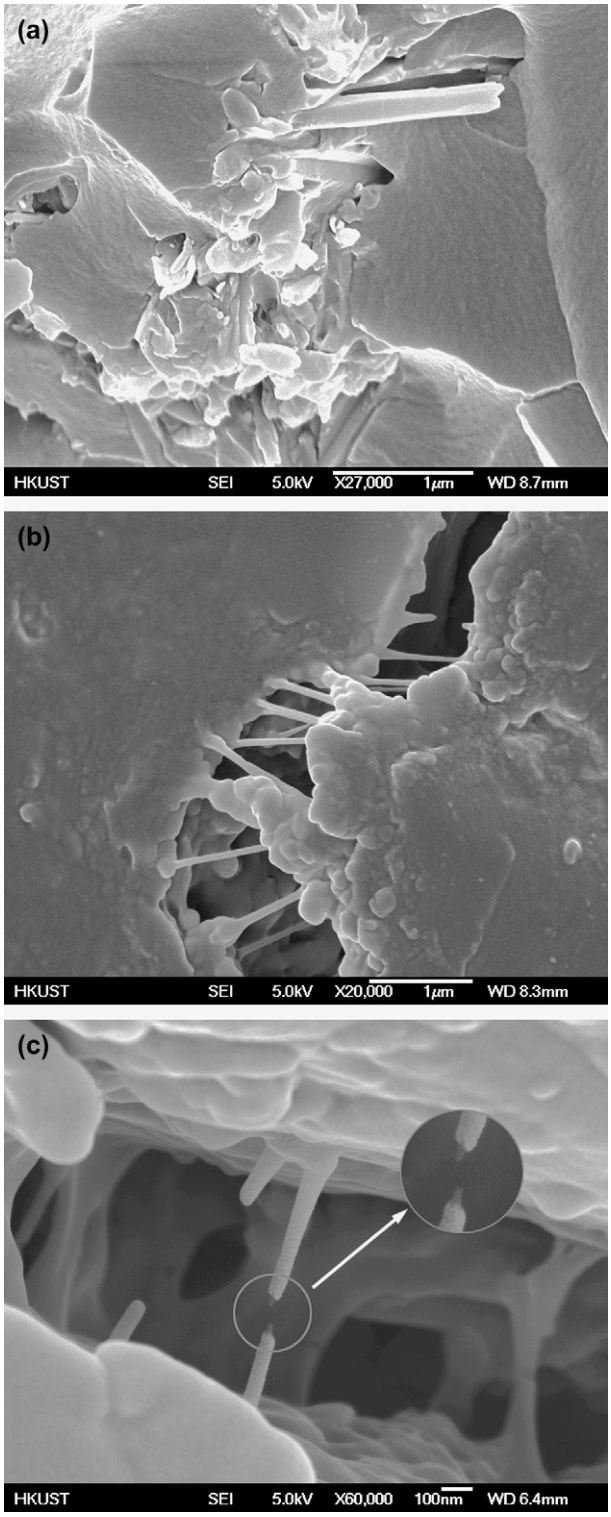

Fig. 9. SEM micrographs taken on the fracture surfaces of the nanocomposites with 2.3 wt% halloysite showing: (a) nanotube debonding/pull-out, (b) nanotube bridging, and (c) nanotube fracture.

fracture behaviour of MWCNTs reported in Ref. [38], the ''sword and sheath'' fracture was also found with the HNTs, as indicated by the enlarged micrograph in Fig. 9c. Clearly, before the final rupture of the HNTs, the inner layers of the HNTs were pulled out after the outer layers fractured. This is due to that the van der Waals actions among the nanotube layers are weaker than the bonding strength with the matrix [39]. It is easy to understand that the formation of the micro-cracks will absorb a large amount of fracture energy because the number of the micro-cracks formed in the brittle matrix under impact is massive. This massive micro-cracking mechanism is very much like the massive crazing mechanism proposed by Bucknall et al. [3]. In addition, since the micro-cracks were bridged by rigid and strong nanotubes, tractions would shield the crack tip and slow down the crack growth, too. Furthermore, nanotube pull-out and breakage associated with the micro-crack opening will also consume additional energy.

To understand the correlations between the micro-cracking, the nanotube bridging/pull-out/breaking and the main crack propagation, the deformation zone ahead of an arrested crack tip in the nanocomposites was examined by SEM and the SEM micrographs are shown in Figs. 10 and 11. Obviously, the running crack had been stopped by a damage zone, circled as Damage Zone 1 in Fig. 10, and deflected downwards and eventually arrested by another damage zone, i.e. Damage Zone 2 in Fig. 10. Both damage zones are in white color while the surrounding matrix is in grey color. The white color is a result of stress-whitening effect associated with a large number of micro-cracks formed inside the damage zones. This is evidenced by the enlarged SEM micrograph of the Damage Zone 1, see Fig. 11. It is also noted in the SEM study that the size, shape and the estimated nanotube population of the damaged zones are in the same range as those of the HNT-rich regions defined in Section 3.1 – morphology of the nanocomposites.

Given all the discussed findings, the toughening mechanisms responsible for the substantially improved impact strength are proposed as follows. Fracture mechanics analysis shows that when a notched specimen is impact loaded, a triaxial tensile stress field builds up at the notch tip. The materials within certain range ahead of the crack tip are in plane-strain condition and subjected to a dilatation stress field, which promotes the formation of micro-cracks or crazes. In the present

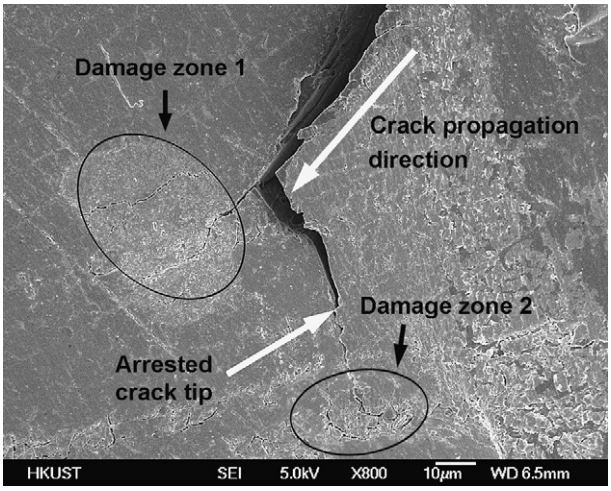

Fig. 10. SEM micrograph of the arrested crack tip of a nanocomposite with 2.3 wt% halloysite.

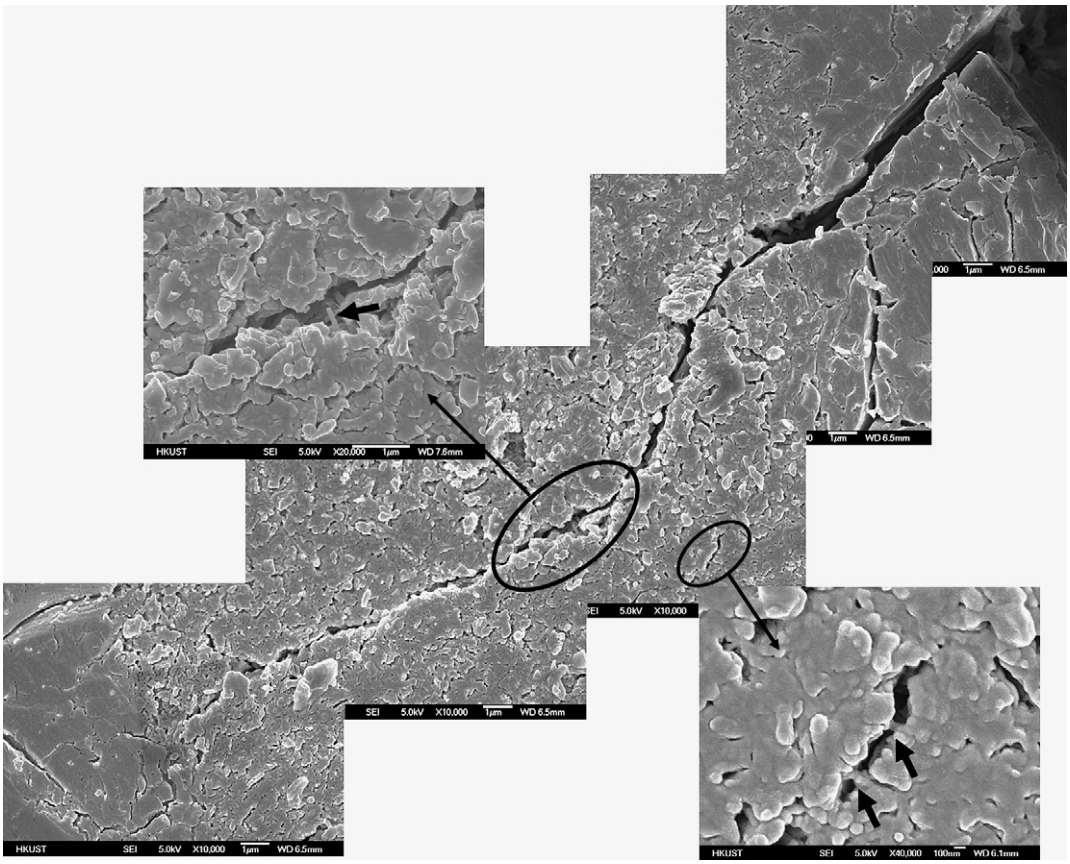

Fig. 11. Enlarged SEM micrographs of Damage Zone 1 in Fig. 10.

study, the morphology of the nanocomposites has two phases, an HNT-rich particle phase embedded in a continuous epoxy-rich phase. When a pre-cracked specimen is loaded above the critical stress, the crack will propagate and keep growing in the direction perpendicular to the loading stress until it encounters the HNT-rich particles. The dilatation stresses and the stress concentration effect from the nanotubes will create a great deal of micro-cracks inside the HNT-rich particles. However, due to the high HNT content, the micro-cracks will soon be stabilized by the crack bridging of neighboring nanotubes without developing into large-sized cracks. This micro-cracking process eventually turns the HNT-rich particles into damage zones in white color. Because of the high energy dissipation of micro-crack formation and nanotube bridging/pull-out/breaking, the HNT-rich particles appear to be tough and strong. The running crack is therefore pinned or deflected or even arrested by the HNT-rich particles, i.e. the damage zones, as demonstrated by Figs. 10 and 11.

In summary, the energy dissipating events observed in the fracture of the epoxy/HNT nanocomposites in the current work include micro-cracking, nanotube bridging/pull-out/breaking and main crack deflection. Although crack deflection results in a more tortuous crack path, hence larger fracture surface area, the contribution from crack deflection to impact strength is marginal. The formation of numerous micro-cracks together with nanotube bridging/pull-out/breaking is believed to be the dominant mechanisms that dissipate tremendous fracture energy and lead to massive enhancement in impact strength of the epoxy/HNT nanocomposites. In line with this proposal, it is suggested that the two-phase structure of the nanocomposite may be necessary in realizing the toughening mechanisms because the HNT-rich particles (the damaged zones) play an important role in stopping the running crack. Moreover, since the formation of massive micro-cracks and nanotube bridging are two key elements of the toughening story, HNT toughening may only be applicable to brittle polymers, such as epoxy, PMMA and PS, of which the yield strength is higher than their fracture strength, thus, micro-cracking takes place before matrix yielding. Blending HNTs with ductile polymers such as PE or PP may not benefit its impact toughness because crack tip blunting due to matrix shear yielding makes HNT bridging impossible.

4. Conclusion

Epoxy nanocomposites with high impact strength were successfully prepared using halloysite nanotube as the impact modifier without scarifying flexural modulus, strength and thermal stability. Microstructure of halloysite nanotubes is disclosed by SEM and TEM. A two-phase structure, namely an HNT-rich particle phase and an epoxy-rich matrix phase, was found in the epoxy/HNT nanocomposites. The underlying toughening mechanisms responsible for the unusual 400% increase in impact strength were investigated and identified as

massive micro-cracking, nanotube bridging/pull-out/breaking and crack deflection. The former two are proposed as the dominant mechanisms that dissipate extensive impact energy. Given the proposed toughening mechanisms, it is further suggested that the HNT toughening may only be applicable to brittle polymers. Blending HNTs with ductile polymers may not benefit their impact strength due to matrix yielding taking place prior to matrix cracking and crack tip blunting.

The significance of this work is twofold. Firstly, it demonstrates that considerable toughening is obtainable without matrix plastic deformation; hence, brittle polymers can be toughened substantially without scarifying other properties. This makes a noticeable contribution to the existing toughening theory. Secondly, since HNT is abundant, inexpensive and its polar surface can be readily modified, it is a potential alternative to expensive CNT in nanocomposite manufacture, if mechanical property is of concern.

Acknowledgements

The authors thank Hong Kong Research Grant Council for financial support to this project (HKUST 6198/03E). The assistance from the Materials Characterization and Preparation Facility (MCPF) and Advanced Engineering Materials Facility (AEMF) in the Hong Kong University of Science and Technology are highly appreciated. We are grateful to Imerys Tableware New Zealand Limited for halloysite sample supply.

References

[1] Bucknall CB, Smith RR. Polymer 1965;6:437.
[2] Newman S, Strella S. J Appl Polym Sci 1965;9:2297.
[3] Bucknall CB, Clayton D, Keast WE. J Mater Sci 1972;7:1443.
[4] Pearson RA, Yee AF. J Mater Sci 1986;21:2475.
[5] Kinloch AJ, Shaw SJ, Tod DA, Hunston DL. Polymer 1983;24:1341.
[6] Ratna D. Polymer 2001;42:4209.
[7] Okamoto Y. Polym Eng Sci 1983;23:222.
[8] Pearson RA. In: Riew CK, Kinloch AJ, editors. Toughened plastics I: science and engineering. Washington, DC: ACS; 1993. p. 405.
[9] Nakamura Y, Yamaguchi M, Okubo M, Matsumoto T. Polymer 1991; 32:2976.
[10] Lee J, Yee AF. Polymer 2000;41:8363.
[11] Ratna D, Varley R, Singh Raman RK, Simon GP. J Mater Sci 2003; 38:147.
[12] Johnsen BB, Kinloch AJ, Taylor AC. Polymer 2005;46:7352.
[13] Chan C-M, Wu JS, Li JX, Cheung Y-K. Polymer 2002;43:2981.
[14] Basara C, Yilmazer U, Bayram G. J Appl Polym Sci 2005;98:1081.
[15] Wang K, Chen L, Wu JS, Toh ML, He CB, Yee AF. Macromolecules 2005;38:788.
[16] Wang JG, Fang ZP, Gu AJ, Xu LH, Liu F. J Appl Polym Sci 2006;100:97.
[17] Fidelus JD, Wiesel E, Gojny FH, Schulteb K, Wagner HD. Composites Part A 2005;36:1555.
[18] Liu LQ, Wagner HD. Compos Sci Technol 2005;65:1861.
[19] Levis SR, Deasy PB. Int J Pharm 2002;243:125.
[20] Levis SR, Deasy PB. Int J Pharm 2003;253:145.
[21] Kelly HM, Deasy PB, Ziaka E, Claffey N. Int J Pharm 2004;274:167.
[22] Chen B, Liu J, Chen HB, Wu JS. Chem Mater 2004;16:4864.
[23] Wang K, Wang L, Wu JS, Chen L, He CB. Langmuir 2005;21:3613.
[24] Wu JS, Mai Y-W. J Mater Sci 1993;28:6167.
[25] Wu JS, Mai Y-W, Yee AF. J Mater Sci 1994;29:4510.
[26] Wu JS, Yu DM, Mai Y-W, Yee AF. J Mater Sci 2000;35:307.
[27] Yang YX, Zhang NX, Su ZB, Chen ZG, Pan JQ, Cai XC, et al. Clay minerals of China. Beijing: Geological Publishing House; 1994 [chapter 2].
[28] Liu YL, Wei WL, Hsu KY, Ho WH. Thermochim Acta 2004;412:139.
[29] Miyagawa H, Drzal LT. Polymer 2004;45:5163.
[30] Preghenella M, Pegoretti A, Migliaresi C. Polymer 2005;46:12065.
[31] Koerner H, Misra D, Tan A, Drummy L, Mirau P, Vaia R. Polymer 2006;47:3426.
[32] Johnsen BB, Kinloch AJ, Mohammed RD, Taylor AC, Sprenger S. Polymer 2007;48:530.
[33] Bugnicourt E, Galy J, Gérard J-F, Barthel H. Polymer 2007;48:1596.
[34] Ratna D, Becker O, Krishnamurthy R. Polymer 2003;44:7449.
[35] Isik I, Yilmazer U, Bayram G. Polymer 2003;44:6371.
[36] Wetzel B, Haupert F, Friedrich K, Zhang MQ, Rong MZ. Polym Eng Sci 2002;42:1919.
[37] Cooper CA, Cohen SR, Barber AH, Wagner HD. Appl Phys Lett 2002; 81:3873.
[38] Gojny FH, Nastalczyk J, Roslaniec Z, Schulte K. Chem Phys Lett 2003; 370:820.
[39] Yu MF, Lourie O, Dyer MJ, Moloni K, Kelly TF, Rouff RS. Science 2000;287:637.